

NSV 11154 Is a New R Coronae Borealis Star

Nutsinee Kijbunchoo¹, Geoffrey C. Clayton¹, Timothy C. Vieux¹, N. Dickerman¹, T. C. Hillwig², D. L. Welch³, Ashley Pagnotta¹, Sumin Tang⁴, J. E. Grindlay⁴, and A. Henden⁵

ABSTRACT

NSV 11154 has been confirmed as a new member of the rare hydrogen-deficient R Coronae Borealis (RCB) stars based on new photometric and spectroscopic data. Using new photometry, as well as archival plates from the Harvard archive, we have constructed the historical lightcurve of NSV 11154 from 1896 to the present. The lightcurve shows the sudden, deep, irregularly spaced declines characteristic of RCB stars. The visible spectrum is typical of a cool ($T_{eff} \lesssim 5000$ K) RCB star showing no hydrogen lines, strong C_2 Swan bands, and no evidence of ^{13}C . In addition, the star shows small pulsations typical of an RCB star, and an infrared excess due to circumstellar dust with a temperature of ~ 800 K. The distance to NSV 11154 is estimated to be ~ 14.5 kpc. RCB stars are very rare in the Galaxy so each additional star is important to population studies leading to a better understanding the origins of these mysterious stars. Among the known sample of RCB stars, NSV 11154 is unusual in that it lies well above the Galactic plane (5 kpc) and away from the Galactic Center which suggests that its parent population is neither thick disk nor bulge.

¹Department of Physics & Astronomy, Louisiana State University, Baton Rouge, LA 70803 USA; nki-jbu1@tigers.lsu.edu, gclayton@fenway.phys.lsu.edu, tvieux1@tigers.lsu.edu, pagnotta@phys.lsu.edu

²Department of Physics and Astronomy, Valparaiso University, Valparaiso, IN 46383; todd.hillwig@valpo.edu

³Department of Physics and Astronomy, McMaster University, 1280 Main Street West, Hamilton, ON L8S 4M1 Canada; welch@physics.mcmaster.ca

⁴Harvard-Smithsonian Center for Astrophysics, 60 Garden Street, Cambridge, MA 02138; stang@cfa.harvard.edu, josh@head.cfa.harvard.edu

⁵American Association of Variable Star Observers, 49 Bay State Rd., Cambridge, MA 02138; arne@aavso.org

1. Introduction

The R Coronae Borealis (RCB) stars represent an extremely rare class of variable stars (Clayton 1996). They are cool supergiants, which are carbon-rich and hydrogen deficient. Their defining characteristic is large irregular declines in brightness of up to 8 mag caused by the formation of carbon dust. Two scenarios have been suggested which attempt to clarify the origins of the RCB stars, the double degenerate (DD), and the final helium-shell flash (FF). The DD model suggests that RCB stars are formed by the merger of a CO- and a He-white dwarf (WD), and the FF model involves stellar expansion after a helium-shell flash. The high $^{18}\text{O}/^{16}\text{O}$ ratios found in RCB stars favor the DD model. However a few RCB stars show Li in their spectra which may instead favor the FF model (Iben et al. 1996; Clayton 1996).

There could be as many as 3000 RCB stars in the Galaxy based on the numbers found in the Large Magellanic Cloud (LMC), but only 55 have been discovered in the Galaxy so far (Clayton 1996; Alcock et al. 2001; Zaniewski et al. 2005; Tisserand et al. 2008).

About forty-five years ago, Hoffmeister (1966) discovered that NSV 11154 was a variable star (S 9323 Lyr) and suggested that NSV 11154 is a short periodic variable. NSV 11154 was also found to be variable in the ROTSE-I survey with an amplitude of 0.4 mag and it was suggested that NSV 11154 is a long period variable (Akerlof et al. 2000; Wils 2001). Haussler et al. (2009) examined 562 plates, obtained at Sonnenberg Observatory during 1964–1996, and found irregular brightness variations between 13.0 and 17.2 mag. On the basis of the lightcurve, they suggested that NSV 11154 may be an RCB star. In this article, we use newly acquired photometry and spectroscopy to attempt to confirm Haussler et al.’s suggestion that NSV 11154 is indeed an RCB star.

2. OBSERVATIONS AND DATA REDUCTION

The UCAC3 coordinates of NSV 11154 are $\alpha(2000) 18^h 37^m 51^s.254$ $\delta(2000)+47$ deg 23' 23''.45 (Zacharias et al. 2010). The field of NSV 11154 is shown in Figure 1.

The Sonnenberg Plate data, taken by a 40 cm astrograph on blue-sensitive photographic plates (Haussler et al. 2009), were downloaded for use in this study. The blue photographic magnitudes were transformed to Johnson V using, $V - m_{pg} = 0.17 - 1.09(B - V)$ (Arp 1961). The transformed data are plotted in Figures 2 and 4. There were 250 additional plates of the NSV 11154 field dating as far back as 1896, available from the Harvard College Observatory plate archive. These plates have been scanned and photometry was done on the stars as part of the Digital Access to a Sky Century at Harvard (DASCH) program (Grindlay et al.

2009), from the scanning focused in the Kepler field. Note that NSV 11154 is a few degrees outside the Kepler field of view, and there are many more Harvard plates covering this star not scanned yet. The measured magnitudes in the DASCH database were converted from photographic magnitudes to Kepler Input Catalog (Sloan) g magnitudes (Brown et al. 2011). The DASCH data were then converted from g to Johnson V using, $V = g' + 0.12 - 0.56(B - V)$ (Fukugita et al. 1996). The DASCH data used here came from twelve plate series from the archive covering the period 1896-1989, and have average uncertainties of 0.15 mag (Laycock et al. 2010). This will be further improved with photometric corrections now being optimized (Tang et al. 2011, in preparation). The Sonnenberg plates were obtained during 1964-1996 so there is an overlap of roughly twenty years with the DASCH data. The DASCH photometry is listed in Table 1 and is plotted in Figures 2 and 4.

The ROTSE-I Northern Sky Variability Survey (NSVS) detected NSV 11154 as a variable (Akerlof et al. 2000). The photometric data were downloaded from the NSVS archive. The ROTSE-I images are unfiltered and Woźniak et al. (2004) suggest that m_{ROTSE} is equivalent to Johnson V , when it is actually very close to Cousins R (Bernhard et al. 2005). If the relation between m_{ROTSE} and V_T (Woźniak et al. 2004) is combined with the equations to convert from V_T to Johnson V^1 , then the conversion is equivalent to $V = m_{ROTSE} + (V-R)_C = m_{ROTSE} + 0.55$. The converted ROTSE-I photometry still seems to have a systematic shift from the actual Johnson V photometry (see below) of ~ 0.2 mag. The ROTSE-I photometry is listed in Table 2, and is plotted in Figures 2 and 4.

New BVR_CI_C photometry has been obtained with the AAVSO Sonoita Research Observatory (SRO) between 2010 October and 2011 June. The images were obtained with the 35cm C14 OTA (SRO35) and the 50cm f/4 Newtonian (SRO50). The images were flat-fielded and dark subtracted. Aperture photometry was done using DAOPHOT in IRAF. The instrumental BV magnitudes were transformed to standard magnitudes using a photometric BV sequence of the field (5169jnc) provided by the AAVSO. In particular, two stars, 2MASS 18374206+4723474 and 18374814+4724267, were used. These stars are both in the Kepler Input Catalog (Brown et al. 2011). Their Sloan gri magnitudes were transformed to Cousins R and I (Fukugita et al. 1996) and then were used to transform the SRO RI instrumental magnitudes of NSV 11154 to standard R_CI_C magnitudes. The uncertainties are ~ 0.01 - 0.02 mag. The BVR_CI_C photometry is listed in Table 3 and plotted in Figures 3 and 4. In addition, there is also photometry from 2MASS, AKARI, and IRAS for NSV 11154. These data are tabulated in Table 4. The 2MASS data were obtained during a gap between the Sonnenberg and ROTSE-I photometry but the star appears to be at or near maximum light.

¹<http://heasarc.nasa.gov/W3Browse/all/tycho2.html>

Spectra of NSV 11154 were obtained on 2009 August 18 using the 4m telescope at Kitt Peak National Observatory (KPNO) with the RC spectrograph using the BL380 grating which has a resolution of 0.9 \AA . Three consecutive 600s spectra were summed. The spectra were not flux calibrated. The wavelength calibration has an rms uncertainty of about 0.02 \AA . The summed spectrum is plotted in Figure 5 along with the spectrum of a similar RCB star HV 5637 (Alcock et al. 2001).

3. DISCUSSION

The historical NSV 11154 lightcurve, seen in Figure 4 from 1896 to 2011, is fragmentary, but several deep declines are apparent. The last decline detected was in 1996, but the coverage since then has been spotty. No declines are seen in the recent ROTSE-I or SRO photometry. Although the lightcurve data are sparse, NSV 11154 seems to be an active RCB star having frequent declines. There are at least 13 epochs where NSV 11154 is seen 2 mag or more below maximum light. These are listed in Table 5. The characteristic time between declines in RCB stars is typically about 1000 days, but there is a wide range in activity among the RCB stars (Feast 1986; Jurcsik 1996). From the ROTSE-I and SRO lightcurves it can be seen that NSV 11154 pulsates with period of ~ 50 days between 1999-2000, and ~ 40 days in 2010-2011. The pulsations have an amplitude of ~ 0.4 mag.

Figure 5 shows the visible spectrum of NSV 11154 compared to the LMC RCB star HV 5637. The spectrum of NSV 11154 is typical of a cool ($\lesssim 5000 \text{ K}$) RCB star with strong CN and C_2 absorption bands (Clayton 1996; Alcock et al. 2001). There is no sign of either $\text{H}\beta$ or $\text{H}\gamma$ indicating extreme hydrogen deficiency. The CH band at 4300 \AA is also absent. In addition, the $^{12}\text{C}^{13}\text{C}$ band at 4744 \AA is weak or absent, while the $^{12}\text{C}^{12}\text{C}$ band at 4737 \AA is very strong indicating a high ^{12}C to ^{13}C ratio. This is typical of most RCB stars. NSV 11154 lies well out of the Galactic plane at $b^{II} = +21^\circ 8$, and so the estimated foreground extinction is quite small, $E(\text{B-V}) = 0.07 \text{ mag}$ (Schlegel et al. 1998). NSV 11154 has an observed $(\text{B-V})=1.1 \text{ mag}$ which is consistent with it being $\lesssim 5000 \text{ K}$ and lightly reddened (Lawson et al. 1990).

The measured colors of NSV 11154, $\text{B-V} = 1.1$ and $\text{V-I} = 1.2$, assuming little or no reddening, are consistent with an absolute magnitude of $M_V = -4 \text{ mag}$ (Alcock et al. 2001; Tisserand et al. 2009). Then, if the foreground extinction is $A_V \sim 0.2 \text{ mag}$, the distance to NSV 11154 is $14.5 \pm 1.5 \text{ kpc}$. This also implies that NSV 11154 is 5.4 kpc above the Galactic plane. Most RCB stars are within 2 kpc of the plane (Zaniewski et al. 2005). Only two other RCB stars in the Galaxy, UX Ant and U Aqr, are as far above or below the plane as NSV 11154. Also, most RCB stars are seen toward the Galactic center, but NSV 11154 has l^{II}

= 76°. NSV 11154 lies well away from the extended body of the Sagittarius Dwarf Galaxy (Majewski et al. 2003).

Using the photometry in Table 4, an SED for NSV 11154 has been plotted in Figure 6. This SED can be fit very well by two blackbodies with temperatures of 4500 and 800 K corresponding to the RCB star itself and its circumstellar dust, respectively. The RCB dust shells typically have temperatures range from 600 K to 900 K (Walker 1985).

4. Summary

The suggestion of Haussler et al. (2009), on the basis of the lightcurve, that NSV 11154 is an RCB star was correct. The spectrum and colors of NSV 11154 show it to be a cool ($\lesssim 5000$ K) RCB star. Archival photometry as well as new BVR_CI_C photometry have been collected giving a historical lightcurve from 1896 to the present. The new photometry shows that NSV 11154 has a semi-regular pulsation period of 40-50 d with an amplitude of 0.4 mag. Although the lightcurve is fragmentary, NSV 11154 has had a number of deep declines showing it to be an active RCB star. The star also displays a significant IR excess indicating the presence of dust with $T \sim 800$ K, which is typical of RCB stars.

Only 55 other RCB stars are known in the Galaxy, so each addition is important to population studies, which will help us to better understand the origins of these mysterious stars. NSV 11154 lies well above the Galactic plane quite different from most other RCB stars which seem to fit into an old disk or bulge population. This may favor the final flash model for this star since the higher stellar density of the Galactic center region is more conducive to formation of RCB stars by the double degenerate scenario. Despite being very rare, RCB stars may be a key to understanding the late stages of stellar evolution. Their measured isotopic abundances imply that many RCB stars are produced by the mergers of double degenerate white dwarfs, which may be the low-mass counterparts of the more massive mergers thought to produce type Ia supernovae. Therefore, knowing the population of RCB stars in the Galaxy will help determine the frequency of these white dwarf mergers.

This paper used data from Digital Access to a Sky Century at Harvard (DASCH) supported by NSF grants AST-0407380 and AST-0909073, as well as by the *Cornel and Cynthia K. Sarosdy Fund*.

REFERENCES

- Akerlof, C., et al. 2000, *AJ*, 119, 1901
- Alcock et al. 2001, *ApJ*, 554, 298
- Arp, H. 1961, *ApJ*, 133, 869
- Bernhard, K., Lloyd, C., Berthold, T., Kriebel, W., & Renz, W. 2005, *IBVS*, 5620, 1
- Brown, T. M., Latham, D. W., Everett, M. E., & Esquerdo, G. A. 2011, arXiv1102.0342B
- Clayton, G. C. 1996, *PASP*, 108, 225
- Feast, M. W. 1986, *IAU Colloq.* 87, 128, p. 151
- Fukugita, M., Ichikawa, T., Gunn, J. E., Doi, M., Shimasaku, K., & Schneider, D. P. 1996, *AJ*, 111, 1748
- Grindlay, J., Tang, S., Simcoe, R., Laycock, S., Los, E., Mink, D., Doane, A., & Champine, G. 2009, *ASP Conf. Ser.*, 410, 101
- Haussler, K., Berthold, T., & Kroll, P. 2009, *IBVS*, 5890, 1
- Hoffmeister, C. 1966, *Astronomische Nachrichten*, 289, 139
- Iben, I. J., Tutukov, A. V., & Yungelson, L. R. 1996, *ApJ*, 456, 750
- Jurcsik, J. 1996, *Acta Astronomica*, 46, 325
- Lawson, W. A., Cottrell, P. L., Kilmartin, P. M., & Gilmore, A. C. 1990, *MNRAS*, 247, 91
- Laycock, S., Tang, S., Grindlay, J., Los, E., Simcoe, R., & Mink, D. 2010, *AJ*, 140, 1062
- Majewski, S. R., Skrutskie, M. F., Weinberg, M. D., & Ostheimer, J. C. 2003, *ApJ*, 599, 1082
- Schlegel, D. J., Finkbeiner, D. P., & Davis, M. 1998, *ApJ*, 500, 525
- Tisserand, P., et al. 2009, *A&A*, 501, 985
- Tisserand et al. 2008, *A&A*, 481, 673
- Walker, H. J. 1985, *A&A*, 152, 58
- Wils, P. 2001, *IBVS*, 5134, 1

Woźniak, P. R., et al. 2004, AJ, 127, 2436

Zacharias, N., et al. 2010, AJ, 139, 2184

Zaniewski, A., Clayton, G. C., Welch, D. L., Gordon, K. D., Minniti, D., & Cook, K. H.
2005, AJ, 130, 2293

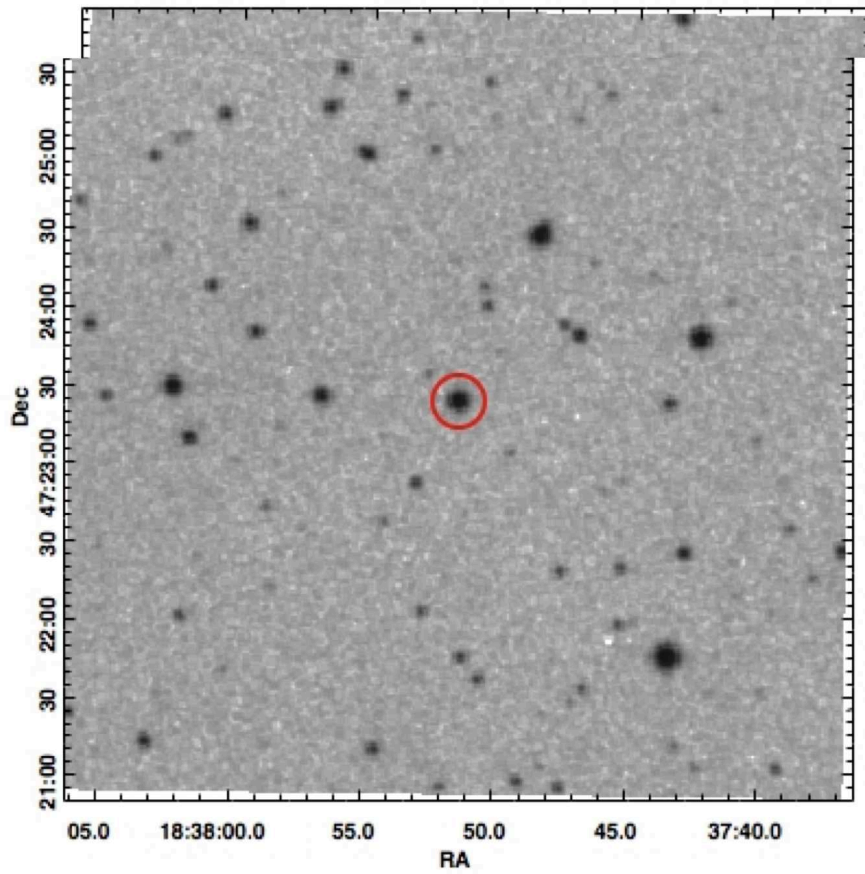


Fig. 1.— Identification chart for NSV 11154 from a POSS-II N plate obtained 1992 June 18. The field is 5'x 5'. The coordinates are J2000.0. North is up and East is to the left.

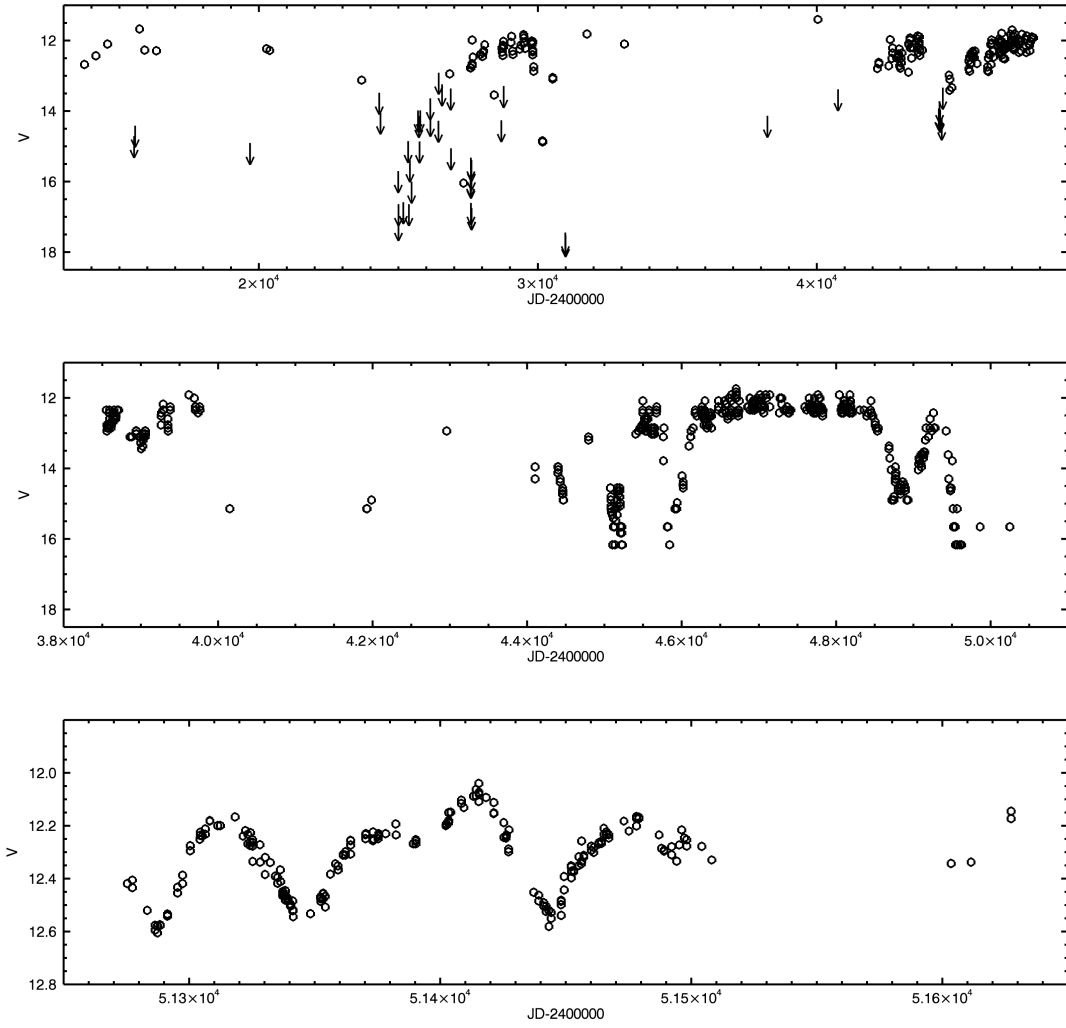


Fig. 2.— V-band lightcurves of NSV 11154. Top: DASCH plate photometry and upper limits (arrows). Middle: Sonneberg plate photometry . Bottom: ROTSE-I photometry.

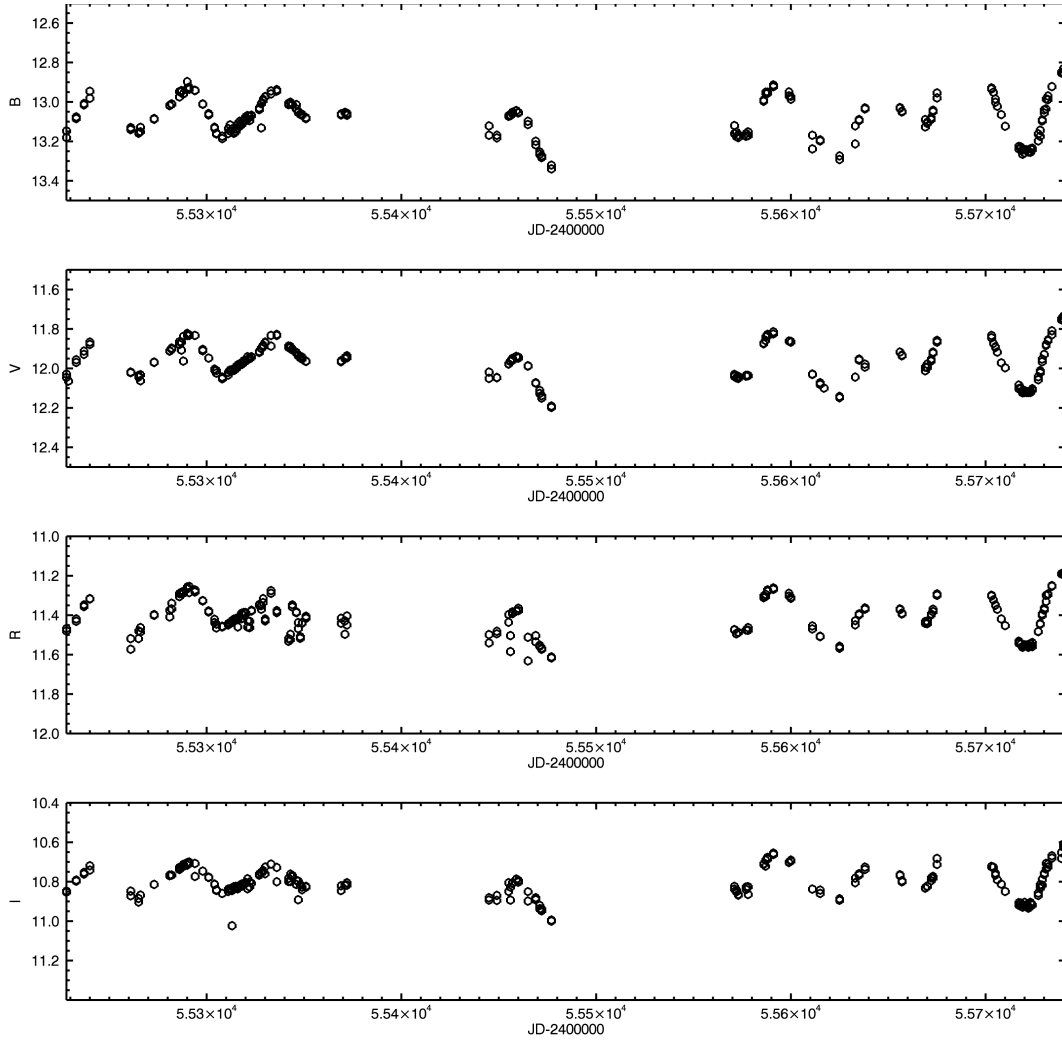


Fig. 3.— SRO lightcurves of NSV 11154. The four panels from the top are B, V, R_C and I_C plotted vs JD.

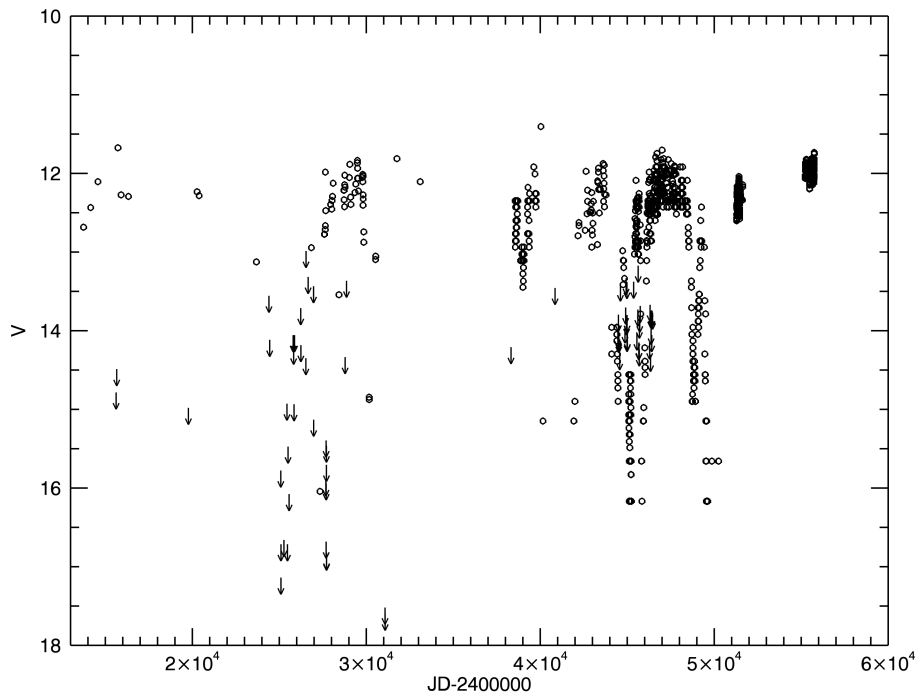


Fig. 4.— Historical lightcurve of NSV 11154 from 1896-2011. Symbols are the same as in Figure 2. Several deep declines are detected.

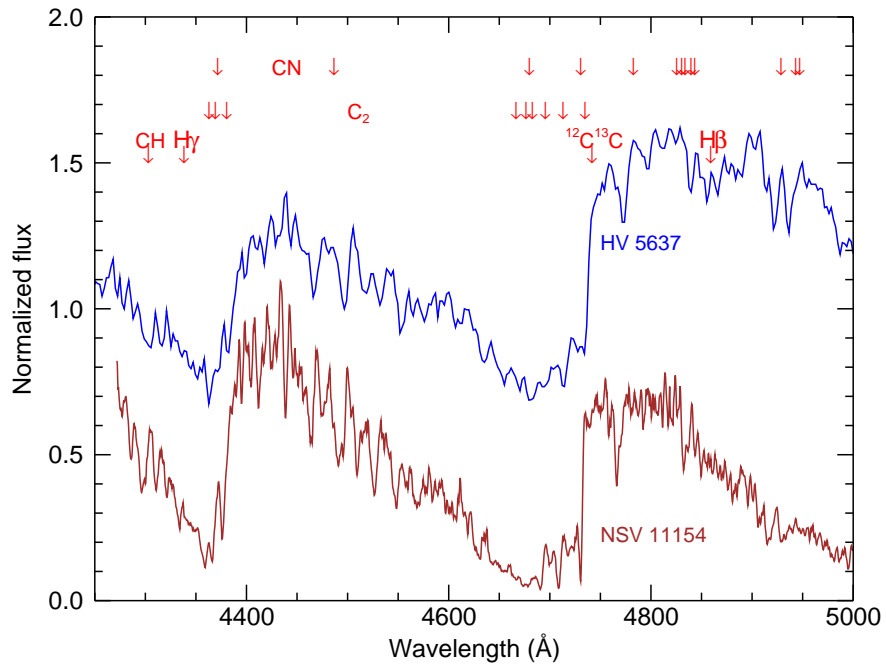


Fig. 5.— The spectrum of NSV 11154, together with the spectrum of HV 5637 a known cool RCB star, for comparison. Note the absence of hydrogen, the strong CN and C₂ bands, and the absence of ¹³C. The spectrum of NSV 11154 is typical for a cool ($\lesssim 5000$ K) RCB star.

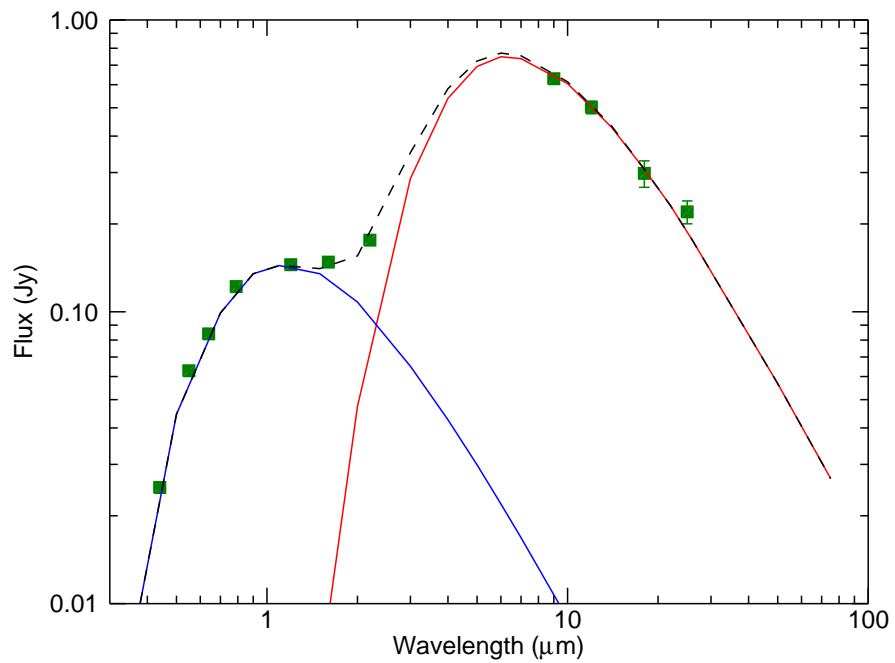


Fig. 6.— The SED of NSV 11154 showing the photometry listed in Table 4 (filled squares). Two blackbodies representing the star and the dust shell, 4500 K (blue line) and 800 K (red line), have been fit to the data. The dashed line is the sum of the two blackbodies.

Table 1. DASCH Photometry

JD	V
2413740.74	12.7
2414154.68	12.4
2414569.61	12.1
2415150.74	>14.8
2415186.80	>14.5
2415717.46	11.7
2415901.67	12.3
2416323.76	12.3
2419306.50	>15.0
2420270.83	12.2
2420385.57	12.3
2423680.54	13.1
2423937.79	>13.6
2423981.69	>14.2
2424618.50	>15.8
2424624.50	>17.2
2424626.50	>16.8
2424800.50	>16.7
2424971.50	>15.0
2424999.50	>16.8
2425035.50	>15.5
2425096.50	>16.1
2425327.87	>14.1
2425354.82	>14.3
2425380.75	>15.0
2425408.72	>14.1
2425765.68	>13.8
2425771.69	>14.2
2426059.88	>14.4
2426067.85	>13.0
2426188.62	>13.4

Table 1—Continued

JD	V
2426498.70	>13.5
2426507.78	>15.2
2426837.79	12.9
2427210.78	>15.9
2427222.74	>15.4
2427225.75	>16.0
2427225.80	>16.7
2427241.75	>15.5
2427241.79	>15.7
2427246.74	>16.9
2427246.79	>16.9
2427334.63	16.0
2427581.70	12.8
2427597.75	12.8
2427640.62	12.7
2427640.76	12.7
2427642.63	12.0
2427668.61	12.5
2427938.73	12.4
2428011.70	12.5
2428023.60	12.3
2428052.56	12.3
2428089.52	12.1
2428314.80	>14.4
2428397.59	>13.4
2428428.57	13.5
2428701.76	12.2
2428717.69	12.3
2428721.68	12.2
2428743.66	12.4
2428749.64	12.1

Table 1—Continued

JD	V
2428760.59	12.0
2428774.63	12.2
2429027.81	12.1
2429052.78	11.9
2429090.71	12.3
2429104.60	12.4
2429344.87	12.2
2429394.81	12.1
2429483.67	11.9
2429485.66	11.8
2429488.61	12.1
2429499.61	11.9
2429521.55	12.1
2429547.52	12.2
2429759.81	12.1
2429787.76	12.0
2429788.75	12.1
2429810.67	12.4
2429810.74	12.0
2429812.64	12.3
2429813.63	12.3
2429846.60	12.7
2429847.64	12.9
2430163.68	14.8
2430167.78	14.9
2430529.77	13.1
2430531.72	13.1
2430608.61	>17.6
2430616.59	>17.6
2431759.51	11.8
2433098.67	12.1

Table 1—Continued

JD	V
2437851.91	>14.2
2440031.74	11.4
2440383.73	>13.5
2442164.78	12.8
2442217.70	12.7
2442219.69	12.6
2442574.75	12.7
2442624.62	12.0
2442684.52	12.5
2442713.49	12.4
2442714.49	12.2
2442849.89	12.5
2442902.80	12.5
2442923.80	12.4
2442923.82	12.5
2442932.74	12.5
2442951.74	12.2
2442964.72	12.7
2442992.70	12.8
2443010.66	12.5
2443020.61	12.6
2443050.59	12.4
2443280.77	12.9
2443289.71	12.1
2443303.77	12.1
2443335.67	12.0
2443339.64	11.9
2443347.67	12.2
2443395.64	12.5
2443421.55	12.2
2443448.48	12.2

Table 1—Continued

JD	V
2443613.79	12.0
2443613.84	11.9
2443630.80	12.4
2443640.72	12.2
2443659.74	12.1
2443659.77	12.0
2443670.74	11.9
2443688.74	12.4
2443690.75	12.3
2443777.59	12.3
2443994.76	>14.0
2444024.74	>14.1
2444024.77	>13.8
2444045.67	>14.1
2444045.72	>14.1
2444099.59	>14.3
2444140.56	>13.5
2444402.74	>14.0
2444439.68	>13.7
2444465.65	>13.4
2444494.57	>13.9
2444514.52	>13.4
2444522.51	>14.1
2444522.58	>13.8
2444539.48	>14.1
2444732.76	13.0
2444756.79	13.4
2444761.74	13.1
2444836.61	13.3
2444898.48	>13.4
2445027.89	>12.8

Table 1—Continued

JD	V
2445089.75	>14.1
2445107.77	>12.6
2445139.70	>13.8
2445162.64	>13.2
2445195.64	>14.2
2445207.61	>14.2
2445223.59	>14.3
2445232.58	>13.9
2445253.53	>13.8
2445281.49	>13.7
2445442.80	12.6
2445442.86	12.8
2445467.77	12.5
2445472.72	12.9
2445494.70	12.7
2445518.70	12.4
2445525.66	12.6
2445550.67	12.4
2445581.61	12.5
2445587.57	12.3
2445606.55	12.4
2445636.52	12.5
2445665.45	12.3
2445742.90	12.7
2445819.80	>14.2
2445846.75	>13.7
2445872.68	>14.3
2445883.69	>13.8
2445905.70	>14.0
2445930.62	>13.8
2445939.61	>14.1

Table 1—Continued

JD	V
2445960.57	>13.8
2445989.51	>13.8
2446114.92	12.9
2446117.92	12.7
2446140.89	12.5
2446150.88	12.9
2446173.80	12.4
2446206.73	12.4
2446231.74	12.1
2446236.81	12.7
2446260.70	12.0
2446270.69	12.1
2446316.62	12.3
2446325.57	12.5
2446326.58	12.3
2446523.83	12.2
2446532.84	12.1
2446532.87	12.0
2446533.70	12.4
2446553.76	12.4
2446564.76	12.0
2446584.80	12.3
2446612.73	12.2
2446619.64	11.8
2446622.81	12.4
2446637.62	12.0
2446668.57	12.5
2446681.60	12.3
2446727.49	12.3
2446732.47	12.2
2446735.52	12.5

Table 1—Continued

JD	V
2446763.48	12.2
2446853.89	12.2
2446915.78	12.1
2446946.69	11.8
2446965.69	12.0
2446970.72	12.1
2446975.76	12.1
2446999.68	11.7
2447026.67	12.2
2447031.61	11.9
2447064.57	12.3
2447082.55	12.2
2447085.50	12.0
2447090.53	11.8
2447210.91	12.0
2447238.86	12.1
2447243.87	12.3
2447270.81	12.0
2447277.83	12.0
2447294.80	12.1
2447296.77	12.0
2447319.73	12.3
2447353.69	11.8
2447469.49	12.0
2447480.51	12.0
2447504.46	12.3
2447525.45	11.9
2447596.90	12.1
2447626.87	12.1
2447628.75	12.3
2447651.79	12.0

Table 1—Continued

JD	V
2447689.79	12.0
2447706.70	11.9
2447762.59	11.9

^aThe uncertainties are ~ 0.15 mag.

Table 2. ROTSE-I Photometry

JD	V	σ_V
2451275.3466	12.42	0.02
2451277.3501	12.41	0.01
2451277.3511	12.43	0.02
2451283.2551	12.52	0.02
2451286.3526	12.60	0.02
2451286.3537	12.58	0.02
2451287.3534	12.58	0.01
2451287.3544	12.61	0.02
2451288.3543	12.58	0.01
2451288.3553	12.58	0.01
2451291.3096	12.54	0.02
2451291.3106	12.54	0.02
2451295.3537	12.46	0.02
2451295.3547	12.43	0.02
2451297.3717	12.39	0.02
2451297.3727	12.42	0.02
2451300.3668	12.28	0.02
2451300.3678	12.30	0.02
2451304.2117	12.25	0.01
2451304.3632	12.23	0.01
2451304.3642	12.24	0.01
2451305.2125	12.24	0.01
2451306.3649	12.23	0.01
2451306.3659	12.21	0.01
2451308.2150	12.18	0.02
2451308.2160	12.18	0.02
2451311.3743	12.20	0.01
2451312.3647	12.20	0.01
2451318.2341	12.17	0.03
2451321.3776	12.24	0.01
2451322.3752	12.22	0.01

Table 2—Continued

JD	V	σ_V
2451323.3634	12.23	0.01
2451323.3644	12.27	0.01
2451324.2246	12.26	0.02
2451324.2256	12.28	0.02
2451324.3714	12.23	0.01
2451325.2260	12.25	0.03
2451325.2263	12.26	0.03
2451325.2809	12.34	0.03
2451325.2812	12.28	0.03
2451328.1871	12.27	0.04
2451328.2430	12.34	0.03
2451330.1883	12.39	0.03
2451330.2451	12.32	0.03
2451332.2462	12.34	0.03
2451334.2310	12.39	0.01
2451335.2316	12.42	0.01
2451335.2326	12.40	0.01
2451336.2332	12.37	0.02
2451336.3892	12.41	0.01
2451337.2327	12.47	0.01
2451337.2337	12.45	0.01
2451337.3897	12.46	0.01
2451337.3907	12.45	0.01
2451338.2332	12.45	0.01
2451338.2342	12.48	0.02
2451338.3902	12.47	0.01
2451338.3912	12.46	0.01
2451339.2336	12.49	0.02
2451339.2347	12.48	0.02
2451339.3906	12.48	0.01
2451339.3916	12.48	0.01

Table 2—Continued

JD	V	σ_V
2451340.2274	12.50	0.01
2451340.2284	12.50	0.01
2451340.3943	12.50	0.01
2451341.2325	12.49	0.01
2451341.2335	12.52	0.01
2451341.3894	12.55	0.02
2451341.3904	12.52	0.02
2451348.3089	12.53	0.02
2451348.3099	12.53	0.02
2451352.2334	12.47	0.02
2451352.2344	12.47	0.02
2451352.3862	12.49	0.01
2451352.3872	12.48	0.01
2451353.2829	12.48	0.02
2451353.2833	12.46	0.02
2451353.3387	12.46	0.02
2451354.1960	12.47	0.03
2451354.1964	12.51	0.03
2451356.2066	12.38	0.03
2451358.1957	12.35	0.03
2451359.2428	12.37	0.03
2451359.2431	12.35	0.03
2451359.2995	12.37	0.02
2451361.2545	12.31	0.03
2451361.2548	12.31	0.03
2451362.1948	12.31	0.02
2451362.1951	12.30	0.02
2451364.2336	12.26	0.02
2451364.2339	12.31	0.02
2451364.2920	12.27	0.02
2451364.2924	12.26	0.02

Table 2—Continued

JD	V	σ_V
2451370.2307	12.23	0.01
2451370.2317	12.25	0.01
2451370.3866	12.23	0.02
2451373.2314	12.22	0.01
2451373.2324	12.26	0.01
2451373.3873	12.25	0.01
2451375.2303	12.25	0.01
2451375.2313	12.24	0.01
2451375.3784	12.23	0.01
2451375.3794	12.23	0.01
2451378.2265	12.23	0.01
2451382.2217	12.19	0.02
2451382.3797	12.24	0.01
2451389.2382	12.27	0.03
2451390.1794	12.26	0.02
2451390.1797	12.26	0.02
2451390.2375	12.25	0.02
2451390.2378	12.27	0.02
2451402.2079	12.20	0.01
2451402.3650	12.20	0.01
2451402.3660	12.19	0.01
2451403.2073	12.19	0.01
2451403.2083	12.19	0.01
2451403.3623	12.18	0.01
2451403.3633	12.15	0.01
2451404.2075	12.15	0.02
2451408.3525	12.12	0.01
2451408.3535	12.10	0.01
2451409.3985	12.13	0.01
2451413.1923	12.09	0.01
2451414.2447	12.09	0.02

Table 2—Continued

JD	V	σ_V
2451414.2451	12.06	0.02
2451415.3234	12.04	0.03
2451415.3237	12.11	0.03
2451415.3783	12.08	0.04
2451415.3786	12.07	0.03
2451418.2478	12.09	0.03
2451421.2483	12.16	0.02
2451421.3044	12.11	0.02
2451421.3047	12.15	0.02
2451425.2525	12.25	0.02
2451425.2528	12.19	0.02
2451426.1777	12.24	0.01
2451426.1787	12.25	0.01
2451426.3306	12.24	0.01
2451427.1766	12.29	0.01
2451427.1776	12.30	0.01
2451427.3307	12.22	0.02
2451437.2363	12.45	0.02
2451439.2217	12.49	0.02
2451439.2227	12.46	0.02
2451441.1628	12.49	0.02
2451441.1638	12.50	0.02
2451442.1238	12.51	0.02
2451442.1242	12.53	0.02
2451443.2224	12.52	0.03
2451443.2787	12.58	0.03
2451444.1761	12.53	0.03
2451444.1764	12.55	0.03
2451448.1171	12.50	0.02
2451448.1174	12.49	0.02
2451448.1734	12.48	0.03

Table 2—Continued

JD	V	σ_V
2451448.1737	12.54	0.03
2451449.3238	12.39	0.04
2451449.3241	12.44	0.04
2451452.1202	12.35	0.02
2451452.1206	12.36	0.02
2451452.1778	12.37	0.02
2451452.1781	12.40	0.02
2451453.1473	12.37	0.01
2451453.1483	12.38	0.01
2451455.1839	12.32	0.01
2451455.1850	12.35	0.01
2451456.1449	12.35	0.01
2451456.2872	12.26	0.02
2451456.2882	12.34	0.02
2451457.1439	12.32	0.01
2451457.1449	12.31	0.01
2451460.1410	12.28	0.01
2451460.1420	12.29	0.01
2451461.1422	12.28	0.01
2451461.1432	12.30	0.01
2451463.1402	12.27	0.01
2451463.1412	12.27	0.01
2451464.1394	12.26	0.01
2451464.1404	12.27	0.01
2451465.1384	12.21	0.01
2451465.1394	12.23	0.01
2451466.1375	12.22	0.01
2451466.1385	12.23	0.01
2451467.1366	12.25	0.01
2451467.1376	12.23	0.01
2451473.1370	12.18	0.02

Table 2—Continued

JD	V	σ_V
2451475.1170	12.22	0.02
2451478.0896	12.17	0.02
2451478.0899	12.17	0.02
2451478.1469	12.20	0.02
2451479.0895	12.17	0.02
2451479.0899	12.17	0.02
2451487.1219	12.24	0.01
2451488.1225	12.29	0.01
2451489.1209	12.29	0.01
2451489.1219	12.30	0.01
2451492.1627	12.31	0.02
2451492.1637	12.28	0.02
2451494.1619	12.34	0.02
2451495.1624	12.27	0.02
2451496.1600	12.22	0.02
2451497.1566	12.25	0.02
2451498.1561	12.28	0.02
2451498.1571	12.25	0.02
2451504.1516	12.28	0.02
2451508.1178	12.33	0.03
2451603.4437	12.34	0.01
2451611.3877	12.34	0.01
2451627.3378	12.15	0.02
2451627.3382	12.17	0.03

Table 3. SRO Photometry

JD	B	V	R _C	I _C
2455228	13.16	12.04	11.47	10.85
2455229	...	12.07
2455233	13.08	11.96	11.43	10.80
2455237	13.01	11.92	11.35	10.76
2455240	12.96	11.87	11.32	10.73
2455261	13.14	12.02	11.55	10.86
2455265	13.16	12.04	11.50	10.89
2455266	13.14	12.04	11.47	10.87
2455273	13.09	11.97	11.40	10.81
2455281	13.02	11.91	11.39	10.77
2455282	13.01	11.90	11.35	10.77
2455286	12.96	11.87	11.30	10.73
2455287	12.95	11.89	11.29	10.73
2455288	12.96	11.90	11.29	10.72
2455290	12.92	11.83	11.26	10.71
2455291	12.93	11.83	11.27	10.71
2455294	12.94	11.83	11.28	10.74
2455298	13.01	11.91	11.33	10.75
2455301	13.06	11.95	11.38	10.78
2455304	13.13	12.01	11.43	10.81
2455305	13.16	12.02	11.46	10.84
2455308	13.18	12.05	11.46	10.86
2455311	13.15	12.03	11.45	10.84
2455312	13.13	12.01	11.44	10.84
2455313	13.14	12.01	11.43	10.94
2455314	13.16	12.01	11.42	10.83
2455315	13.14	12.00	11.42	10.83
2455316	13.12	11.99	11.44	10.83
2455317	13.11	11.98	11.40	10.82
2455318	13.11	11.98	11.40	10.82
2455319	13.10	11.97	11.39	10.81

Table 3—Continued

JD	B	V	R _C	I _C
2455320	13.09	11.96	11.39	10.81
2455321	13.08	11.95	11.44	10.81
2455322	13.08	11.95	11.45	10.81
2455323	13.07	11.94	11.38	10.81
2455327	13.04	11.92	11.35	10.77
2455328	13.07	11.90	11.36	10.76
2455329	12.99	11.89	11.33	10.75
2455330	12.97	11.87	11.42	10.74
2455333	12.95	11.86	11.28	10.71
2455336	12.94	11.83	11.38	10.76
2455342	13.01	11.89	11.53	10.79
2455343	13.00	11.89	11.51	10.78
2455344	13.01	11.91	11.35	10.77
2455346	13.03	11.92	11.39	10.80
2455347	13.05	11.94	11.45	10.84
2455348	13.06	11.94	11.51	10.82
2455349	13.07	11.95	11.44	10.83
2455351	13.08	11.97	11.41	10.83
2455369	13.06	11.96	11.43	10.83
2455371	13.05	11.95	11.46	10.82
2455372	13.06	11.94	11.43	10.81
2455445	13.15	12.04	11.52	10.89
2455449	13.18	12.05	11.49	10.88
2455455	13.07	11.98	11.42	10.83
2455456	13.07	11.96	11.54	10.86
2455457	13.06	11.95	11.39	10.81
2455459	13.05	11.94	11.38	10.79
2455460	13.06	11.95	11.37	10.80
2455465	13.11	11.99	11.57	10.87
2455469	13.21	12.07	11.52	10.89
2455471	13.26	12.12	11.56	10.93

Table 3—Continued

JD	B	V	R _C	I _C
2455472	13.28	12.14	11.57	10.94
2455477	13.33	12.20	11.61	11.00
2455571	13.15	12.04	11.47	10.83
2455572	13.17	12.05	11.49	10.85
2455573	13.17	12.05	11.49	10.87
2455577	13.17	12.04	11.48	10.83
2455578	13.16	12.04	11.47	10.85
2455586	12.99	11.87	11.31	10.71
2455587	12.95	11.85	11.30	10.71
2455588	12.95	11.83	11.28	10.68
2455591	12.92	11.82	11.27	10.66
2455599	12.96	11.86	11.30	10.70
2455600	12.98	11.87	11.31	10.69
2455611	13.20	12.03	11.46	10.84
2455615	13.20	12.08	11.51	10.85
2455617	...	12.10
2455625	13.28	12.15	11.56	10.89
2455633	13.18	12.05	11.43	10.80
2455635	13.09	11.96	11.40	10.76
2455638	13.03	11.99	11.37	10.73
2455656	13.03	11.92	11.37	10.77
2455657	13.05	11.94	11.39	10.80
2455669	13.11	12.00	11.44	10.83
2455670	13.11	11.99	11.44	10.82
2455672	13.09	11.96	11.40	10.79
2455673	13.05	11.92	11.38	10.78
2455675	12.97	11.86	11.30	10.70
2455703	12.93	11.84	11.30	10.72
2455704	12.95	11.87	11.32	10.73
2455705	12.99	11.89	11.35	10.76
2455706	13.02	11.92	11.37	10.79

Table 3—Continued

JD	B	V	R _C	I _C
2455708	13.06	11.97	11.42	10.81
2455710	13.12	12.00	11.45	10.85
2455717	13.23	12.09	11.54	10.91
2455718	13.23	12.10	11.55	10.92
2455719	13.26	12.12	11.56	10.92
2455720	13.25	12.12	11.55	10.91
2455721	13.24	12.12	11.55	10.92
2455722	13.26	12.12	11.56	10.93
2455723	13.25	12.12	11.55	10.91
2455724	13.24	12.11	11.55	10.92
2455727	13.18	12.05	11.48	10.86
2455728	13.16	12.02	11.45	10.83
2455729	13.09	11.96	11.40	10.80
2455730	13.05	11.93	11.37	10.76
2455731	13.01	11.88	11.32	10.72
2455732	12.98	11.86	11.29	10.72
2455734	12.92	11.82	11.25	10.67
2455739	12.85	11.75	11.19	10.67
2455740	12.84	11.74	11.19	10.62
2455741	12.84	11.74	11.19	10.63

^aThe uncertainties are ~ 0.01 - 0.02 mag.

Table 4. Photometry of NSV 11154

Bands	Flux(Jy)	σ
U	2.50E-02	2.30E-04
V	6.28E-02	1.16E-05
R _C	8.40E-02	7.69E-04
I _C	1.22E-01	1.12E-03
J	1.45E-01	3.00E-03
H	1.48E-01	3.00E-03
K	1.76E-01	2.00E-03
AKARI/9	6.29E-01	1.10E-02
IRAS/12	5.02E-01	2.50E-02
AKARI/18	2.98E-01	3.10E-02
IRAS/25	2.20E-01	1.98E-02

Table 5. Decline Epochs of NSV 11154

JD ^a	Length (d)
2415150	...
2419306	...
2423981	~2525
2427246	...
2428314	...
2430616	...
2437851	...
2440150	~1775
2444099	~375
2445027	>150
2445742	~400
2448682	~375
2449422	>450

^aThe photometry shown in Figures 2 and 3 is fragmentary so the decline epochs and lengths of the declines are best estimates.